# Laser micro-impulse torsion pendulum

**Jing Li (李　静) and Zhiping Tang (唐志平)**

*Key Lab for Mechanical Behavior and Design of Materials (LMBD), Chinese Academy of Sciences;*
*University of Science and Technology of China, Hefei 230027*

Received August 16, 2004

In order to investigate the feasibility regarding micro-satellite posture steering by laser micro-propulsion, a laser torsion pendulum has been set up so as to get first-hand basic physical and mechanical parameters on laser micro-propulsion. The instrumentation consists of the optical, mechanical, and electrical sub-systems. The optical system includes the main beam optics, the measuring optics, and the observation optics. The mechanical system includes the gyration apparatus, transverse translation stage, vertical translator, focal lenses translator, calibration pendulum translator, and vacuum chamber. For the electrical system a computer is used to control stepping motors to drive the above moving apparatuses. With this instrument the calibration experiment and laser ablation experiment have been carried out. The experimental results demonstrate that the instrument has the capacity to measure impulse down to $10^{-8}$ N·s with an error of about 10.4%, which can satisfy the requirement of micro-impulse measurement.

*OCIS codes:* 140.3440, 120.0120, 000.2190.

The rapid advances of technology launching multiple small satellites can reduce the cost, moreover they can form a net to conduct the tasks that an expensive, large satellite cannot accomplish, therefore, developing nano- and pico-satellites with the mass between $1-10$ kg will be a trend for future space-flight. The posture steering impulse for nano- and pico-satellites in orbit is in the order of $10^{-4}-10^{-6}$ N·s. However, the current cold gas thruster can offer the minimum impulse of about 4.5 mN·s, which cannot satisfy the requirement for accurately adjusting the posture of nano- and pico-satellite in the orbit.

The rapid development of high-brightness diode lasers makes the laser micro-thruster possible. The diode laser beam is focused on the target in vacuum by lenses and causes the target material vaporized and even ionized, which provides the micro-thrust[1]. Presently, the main micro-impulse measuring methods are the testing platform method, the piezoelectric momentum method, the interferometric proximeter system (IPS), and the torsion pendulum method, etc.[1−3]. Among the first three methods, IPS is the best one and can measure the impulse as low as $10^{-4}-10^{-5}$ N·s, but it still cannot satisfy the need of smaller impulse measurement. However, the specially designed torsion pendulum can meet this requirement. Phipps *et al.*[1] developed a micro-impulse torsion pendulum by using a fused silica fiber as torsion thread, which can measure impulse to $10^{-10}$ N·s but with an error of ±50% at this tiny impulse.

In order to exactly measure the micro-thrust of laser propulsion and study the physical mechanism, propulsion efficiency, and parameters optimization for laser micro-propulsion, we have developed a set of laser micro-impulse test equipment based on torsion pendulum principle. Besides the laser propulsion impulse, the parameters such as the momentum coupling coefficient, specific impulse, laser plasma eject velocity, etc., can be obtained with the instrument too. Among them, some parameters are measured directly, others can be figured out.

Figure 1 is a schematic diagram of torsion pendulum. The middle of the pendulum is a torsion thread, one end of the crosshead is the target material, the other end is the balance mass. The focused laser beam irradiates on the target material to produce the impulse, which causes target to rotate around the geometric center of the torsion thread. The deflection angle can be read out from

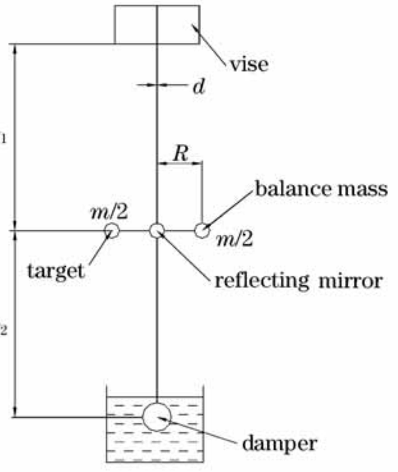

Fig. 1. Schematic diagram of torsion pendulum.

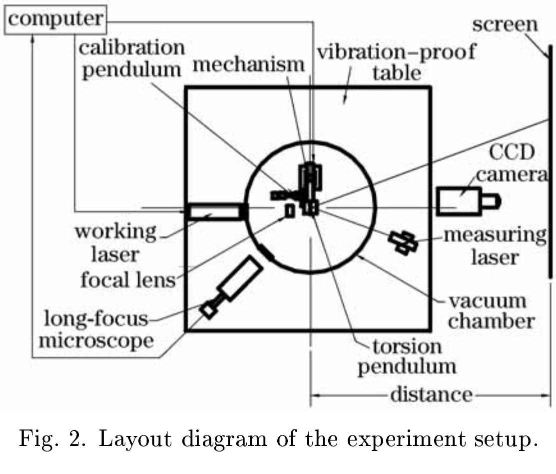

Fig. 2. Layout diagram of the experiment setup.

1671-7694/2005/020076-04　　http://www.col.org.cn

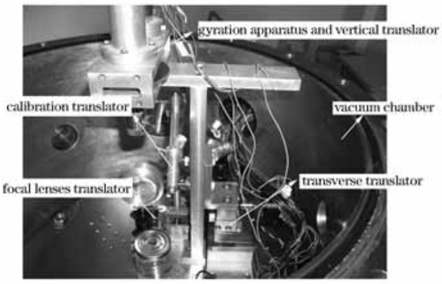

Fig. 3. Picture of the mechanical system.

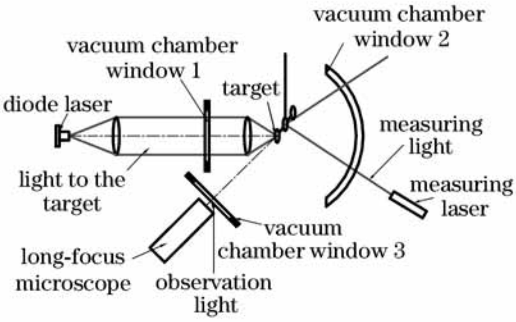

Fig. 4. Layout of optical system.

the measuring laser spot on the screen, which is reflected by a mirror stuck on the crosshead. The makeup and layout of the instrument are shown in Fig. 2.

The mechanical system of the instrument, as shown in Fig. 3, includes the gyration apparatus which is used to adjust the target at different angles to the incident laser beam, the transverse translator and vertical translator which are applied to move target in two directions vertical to the optical axis so as to increase the laser shot number and decrease the time of replacing the target, the focal lenses translator which can adjust the focus position along optical axis to change laser power density, and the calibration translator which is used to calibrate the parameters of $G$, $J$ ($G$ is the shear modulus, and $J$ is the moment of inertia of the torsion thread) and compare them with the theoretical values in order to verify measurement reliability of the instrument. Figure 4 shows the optical system, which includes the main beam optics, measuring optics, and observation optics. In the main beam optics, the diode laser is calibrated and focused on the target in vacuum chamber to produce material vapor or plasma and bring the torsion pendulum to deflect. In the measuring optics, the deflection angle can be read out by He-Ne laser that is reflected by a mirror, in addition, optical lever and reading from distance outside chamber mode are used to improve the resolution of impulse measurement. The observation optics consists of a long-focus microscope, a charge-coupled device (CCD) camera, an image collector, and a computer to measure the position and size of focus on the target, control the movement of the focal lenses, and adjust the focus to proper size. The electric system uses a computer to control the direction and step number of the five stepping motors in the mechanical system and the working time of the diode laser.

The basic measuring parameters are the deflection angle of torsion pendulum ($\theta_0$) and the ablated mass ($\Delta m$), the other important parameters, including the coupling impulse ($P$), the momentum coupling coefficients ($C_\mathrm{m}$), the specific energy ($Q^*$), the exhaust velocity ($V_\mathrm{E}$), and the specific impulse ($I_\mathrm{sp}$), can be calculated by the following equations,

$$\begin{aligned}
\frac{P}{\theta_0} &= \sqrt{\frac{GJ_\mathrm{m}}{L}}, \\
C_\mathrm{m} &= (P/\theta_0)(\theta_0/W), \\
Q^* &= W/\Delta m, \\
V_\mathrm{E} &= C_\mathrm{m}Q^* = gI_\mathrm{sp}. \qquad (1)
\end{aligned}$$

The main technical parameters of the torsion pendulum system are the shear modulus $G$ and the moment of inertia $J$. The value of $GJ$ can be determined by applying a constant force on the pendulum. Figure 5 demonstrates the experimental calibration method. The movement of the calibration translator is controlled by electrical pulses (a single pulse produces a displacement of 8.33 $\mu$m), then the displacement of the hanging point of the small calibration ball is determined by the motor stepping number, which brings the small ball incline and gives the torsion pendulum a horizontal force, from deflection angle $\theta$ the horizontal displacement $x_1$ can be obtained. The relationship between $x_1$, $x_2$, and $x$ at balance position is shown in Fig. 5. From $x_2$ the force applied on the target material can be obtained, so the value of $GJ$. The detailed calculation is given by

$$\begin{aligned}
x &= x_1 + x_2, \\
x_1 &= R\theta, \\
F &= m_\mathrm{eff}gx_2/L_t, \\
\theta &= \theta_\mathrm{b}/2, \\
\frac{1}{L} &= \frac{1}{L_1} + \frac{1}{L_2}, \\
GJ &= FRL/\theta, \qquad (2)
\end{aligned}$$

where $F$ is the force applied on the torsion pendulum by the calibration ball, $L$ is the effective length of torsion pendulum, $m_\mathrm{eff}$ is the mass of the calibration ball, $\theta_\mathrm{b}$ is the measured angle, $\theta$ is the deflection angle of torsion pendulum, other parameters refer to Figs. 1 and 5.

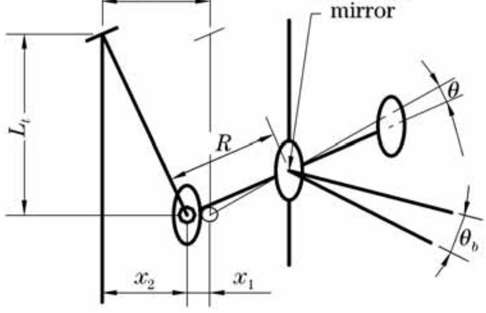

Fig. 5. The schematic diagram of torsion pendulum calibration.

The torsion pendulum uses beryllium bronze as a hanging thread, its geometrical parameters are $d = 58$ $\mu$m, $L = 63$ m, $R = 18$ mm, and $L_{\rm t} = 95$ mm in Fig. 5. $m_{\rm eff} = 229.3$ mg weighed by an analytical balance. From Eq. (2), the value of $GJ$ is obtained as $4.95 \times 10^{-8}$ Pa·m$^4$ based on the experimental calibration. According to the Chinese National Standard GB/T1239.6-92, the shear modulus of beryllium bronze is $G = 4.4\times10^{10}$ Pa, the moment of inertia of the torsion pendulum can be calculated from the geometry as $J = 1.11\times10^{-18}$ m$^4$, then the calculated value is $GJ = 4.88 \times 10^{-8}$ Pa·m$^4$. The relative error between the calibrated and the calculated values is only 1.43%. This demonstrates that the present measuring system has high reliability.

The experimental error expression for the present system can be deduced from the impulse calculation equation as

$$\Delta P = \sqrt{\frac{GJm}{L}} \cdot \Delta\theta + \theta \cdot \left[\frac{1}{2}\sqrt{\frac{GJ}{Lm}} \cdot \Delta m + \frac{1}{2}\sqrt{\frac{GJm}{L^3}}\Delta L + \frac{1}{2}\sqrt{\frac{m}{GJL}}\Delta(GJ)\right]. \quad (3)$$

The reading errors of the parameters in the experiments are estimated as $\Delta\theta = 2.67 \times 10^{-4}$ rad, $\Delta L = 5\times10^{-4}$ m, $\Delta m = 3.64\times10^{-7}$ kg, and $\Delta(GJ) = 7\times10^{-10}$ Pa·m$^4$. Substituting the above reading errors into Eq. (3) yields the following absolute and relative error expressions of the impulse,

$$\Delta P = 1.065 \times 10^{-9} + \theta \times 1.15 \times 10^{-8} (\mathrm{N \cdot s}), \quad (4)$$

$$\frac{\Delta P}{P} = \frac{2.67 \times 10^{-4}}{\theta} + 2.88 \times 10^{-3}. \quad (5)$$

Equations (3) – (5) show that the absolute error increases and the relative error decreases with the increase of impulse (the deflection angle $\theta$). Table 1 lists the measurable impulse range of the torsion pendulum, which is determined by the maximum deflection angle, minimum resolution angle, and the corresponding errors. In the table the maximum relative error is at the bottom of measuring range, which is 10.2%.

**Table 1. Measurable Impulse Range and the Corresponding Errors**

| $\theta$ (rad) | $P$ ($\times10^{-8}$ N·s) | $\Delta P$ ($\times10^{-9}$ N·s) | $\Delta P/P$ (%) |
|---|---|---|---|
| 0.349 | 139.2 | 5.1 | 0.40 |
| 0.0027 | 1.07 | 1.10 | 10.2 |

Black ink-coated paper is used as the target material with the diameter of 13 mm, thickness of 100 $\mu$m, and mass of $1.028 \times 10^{-5}$ kg. A continuous wave (CW) diode laser LDM-0980-002W-5 with the wavelength of 975 nm, divergent angle of 48° × 10°, and rating power of 2 W is used in the experiment. The output power in the experiment is adjusted to 1.6 W, and the laser working time is controlled with a software control switch. In the experiments the target position is adjusted to keep the power density of laser beam on the target steady, which is about $4.5 \times 10^4$ W/cm$^2$. The vacuity in the chamber is about 30 Pa. From Eq. (1) we have

$$P = \sqrt{\frac{GJm}{L}} \cdot \theta. \quad (6)$$

$G$, $J$, $m$, and $L$ are constants, so $P$ has a linear relationship with $\theta$. Increasing the torsion thread diameter, shear modulus, and balance mass or decreasing the effective length of the torsion pendulum can expand the upper range of the impulse measurement. Putting the known data of the presented instrument into Eq. (6) yields

$$P = 3.99 \times 10^{-6}\theta \quad (\mathrm{N \cdot s/rad}). \quad (7)$$

Table 2 lists the laser propulsion experimental data of 10 shots and corresponding calculated results of propulsion parameters. $\tau$ in the table is the working time of diode laser. The minimum impulse is $1.07 \times 10^{-8}$ N·s, which means the instrument can satisfy the requirement on measuring micro-impulse. Figure 6 is a picture of the

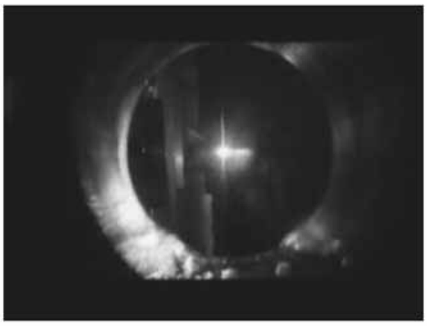

Fig. 6. The photograph of radiation produced by interaction between laser and target material.

**Table 2. Experimental Data and Results**

| Experiment No. | 1 | 2 | 3 | 4 | 5 | 6 | 7 | 8 | 9 | 10 |
|---|---|---|---|---|---|---|---|---|---|---|
| $\tau$ (s) | 0.5 | 0.2 | 0.1 | 0.05 | 0.02 | 0.0125 | 0.01 | 0.005 | 0.002 | 0.001 |
| $\theta$ ($\times10^{-1}$ rad) | 1.07 | 1.02 | 0.77 | 0.385 | 0.22 | 0.18 | 0.21 | 0.12 | 0.048 | 0.027 |
| $P$ ($\times10^{-7}$ N·s) | 4.27 | 4.07 | 3.07 | 1.54 | 0.86 | 0.70 | 0.84 | 0.48 | 0.19 | 0.107 |
| $\Delta m$ ($\times10^{-9}$ kg) | 2.32 | 0.81 | 0.47 | 0.39 | 0.28 | 0.34 | 0.27 | 0.14 | 0.089 | 0.094 |
| $Q^*$ ($\times10^8$ J/kg) | 3.25 | 3.71 | 3.25 | 1.94 | 1.08 | 0.56 | 0.57 | 0.56 | 0.34 | 0.16 |
| $C_{\rm m}$ ($\times10^{-5}$ N/W) | 0.06 | 0.14 | 0.2 | 0.2 | 0.29 | 0.37 | 0.56 | 0.64 | 0.64 | 0.71 |
| $V_{\rm E}$ (m/s) | 184 | 501 | 660 | 396 | 309 | 209 | 318 | 35 | 217 | 113 |
| $I_{\rm sp}$ (s) | 18.8 | 51.1 | 67.4 | 40.3 | 31.6 | 21.3 | 32.5 | 36.0 | 22.1 | 11.6 |

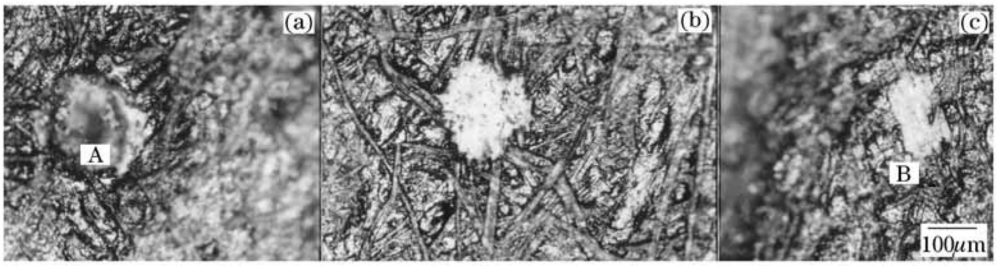

Fig. 7. The photographs of laser ablated material. $\tau = 0.1$ s (a), 0.01 s (b), and 0.001 s (c).

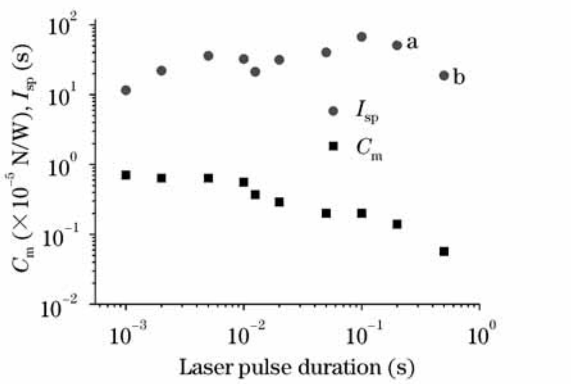

Fig. 8. The relationship between laser working time, momentum coupling coefficients, and specific impulse.

jet produced by the interaction between laser and target material, which is recorded by a cinematograph. Figure 7 shows the photographs of the ablated target material under microscope, the white regions are the ablated areas. The ablated size in Fig. 7(c) is about $150 \times 90$ $\mu$m$^2$. A small dark area in Fig. 7(a) marked with "A" is a burnout area. It can be seen from Fig. 7 that under the constant power density, the ablated area and depth increase gradually with the duration of the laser beam. The specific impulse $I_{\rm sp}$ and momentum coupling coefficient $C_{\rm m}$ in Table 2 versus the laser duration $\tau$ are shown in Fig. 8. It can be seen that the specific impulse is maximum when $\tau = 0.1$ s, then, with decreasing $\tau$ the specific impulse decreases, on the contrary, $C_{\rm m}$ increases gradually. It is found in the experiments that $I_{\rm sp}$ decreases as $\tau$ exceeds 0.1 s, the reason is that the target material in the spot has been burned out, there is no target material for converting the sequent energy into impulse. Therefore, the data of $\tau = 0.5$ and 0.2 s (marks "a" and "b" in the figure) can be regarded as invalid. The changing trend of the data in Fig. 8 agrees with the model prediction for C—H materials in Ref. [4], i.e., under the condition of laser wavelength and power density unchanged, with the increase of the laser duration, the momentum coupling coefficient trends to decline.

In summary, the instrument applies the optical lever principle and the reading mode from outside distance to improve the impulse measuring resolution. The calibration result demonstrates the presented instrument has high measuring reliability. The preliminary laser ablation propulsion experiments are conducted with a diode laser and 100-$\mu$m-thick black paper. The minimum impulse measured in the experiment is $1.07 \times 10^{-8}$ N·s with a relative error of 10.4%, the maximum specific impulse is 67.4 s, the maximum momentum coupling coefficient is $7.09 \times 10^{-6}$ N/W. The results show that as the output of laser power unchanged, with decreasing the working time the specific impulse decreases gradually, but the momentum coupling coefficient increases gradually. The careful calibration, error analysis, and preliminary experimental results described in this article demonstrate the presented torsion pendulum instrument can be used to measure the micro-impulse as low as $1.07 \times 10^{-8}$ N·s.

J. Li's e-mail address is lijing@ustc.edu.cn.

## References

1. C. R. Phipps and J. Luke, Proc. SPIE **4065,** 801 (2000).
2. S. Uchida and M. Bato, in *Proceedings of First International Symposium on Beamed Energy Propulsion* 214 (2002).
3. M. H. Liu, J. W. Sun, Y. L. Chen, and X. D. Cai, Mechanics and Practice (in Chinese) **25,** 9 (2003).
4. C. R. Phipps, Jr., T. P. Turner, R. F. Harrison, G. W. York, W. Z. Osborne, G. K. Anderson, X. F. Corlis, L. C. Haynes, H. S. Steele, K. C. Spicochi, and T. R. King, J. Appl. Phys. **64,** 1083 (1988).